Tuijin Jishu/Journal of Propulsion Technology
ISSN: 1001-4055
Vol. 45 No. 2 (2024)

Numerical Simulation of a Vertical Axis Crossflow Helical Hydrokinetic Turbine

Kumaresan Cunden[1] and Professor Freddie Inambao[2]

[1]PhD *Research Scholar, Department of Mechanical Engineering, University of KwaZulu-Natal, Durban 4000, South Africa*

[2]Professor, Department of Mechanical Engineering, University of KwaZulu-Natal, Durban 4000, South Africa*

Corresponding author: Freddie Inambao[2]*

Abstract : With a growing need for energy and a growing need to decrease dependence on fossil fuel energy production, new methods of energy generation are required. The energy that exists in flowing rivers, ocean currents and various other artificial water channels is considered a viable option of renewable power. These types of systems are still in the infant stages of development as the main focus of renewable energy in recent years has been solar and wind energy harvesting. Recently there has been an increase in research and implementation of vertical axis crossflow hydrokinetic turbines globally. The research data, in conjunction with the ducting system, may be used to extrapolate power capacity for a farm configuration. The research incorporates computational fluid dynamic (CFD) models and supporting numerical modelling to validate the simulation. The simulations were compared to experimental work conducted in the literature. Methodology from previous researchers Kirke (2011) and Khan et al. (2009) was used in the understanding of the turbine system. Methods from Shino et al. (2002) and Sheldahl and Klimas (1981) were used as a basis for the modelling of the turbine. The developed model can effectively predict the hydrodynamic performance of a vertical-axis marine current turbine.

Keywords*:* Double multiple stream tubes, Iterative solver, Ducting systems Introduction

1 Introduction

In the following study, the turbine has a vertical axis orientation. The vertical axis turbine concept was first invented by Darrieus Marie (1931) in 1931. The Darrieus turbine, however, had various problems when it came to extracting energy from the flow medium. One of the key issues stated by Gorlov (1998) was that the Darrieus turbine had torque fluctuations which directly impacted the turbine's efficiency. Gorlov designed a vertical axis turbine which was based on the Darrieus concept. The Gorlov turbine had a helical profile. The helical shape of the blades proved to decrease the torque fluctuations of the blade and subsequently increased the efficiency of the turbine.

The design of vertical axis blades to achieve satisfactory performance begins with the understanding of the hydrodynamic force interaction with the blades. The hydrodynamic forces directly impact the structural loads of the turbine which the rotor will experience. This is highly important in the design process as the life cycle of the rotor is impacted. Blade geometry and orientation also impact the forces on the turbine and efficiency.

The following paper highlights the various methods of analogy that were conducted on the designed helical crossflow turbine. The computational fluid dynamic (CFD) model as well as the different numerical methods which were conducted on the turbine is discussed, on the shrouded system and turbines with different pitch angles.

2 Literature Review

Lazauskas and Kirke (2012) found that tests conducted on straight-blade turbines exhibit relatively low starting torque under loading conditions. They have also observed that unless the blades of the turbine had a helical shape, the turbine vibrates. The vibration is due to the impact of the flow medium on the blades as the blade angles of attack vary due to the turbine rotation. The researchers also state that two key peak forces occur on the

blades as they rotate which are the radial and tangential forces on the blade. The upstream (as the fluid first interacts with the blade) is usually larger compared to the downstream peak which occurs at the outlet side of the turbine. These two components of forces affect the system of generation. The tangential force variation or "torque ripple" affects the transmission load and the radial force variation affects the support structure. If the frequency of the radial force coincides with the natural frequency of the support structure, the harmonics can be highly destructive. Lazauskas and Kirke obtained a memetic algorithm to search for the optimum pitch parameters to increase the efficiency of the turbine. The pitching equation varies the pitch of the blade to obtain the optimum angle of attack so that the losses encored from non-varied angles are diminished. This system is constantly at work changing the pitch of the blades and would require a complex feedback control system.

Khan et al. (2010), performed a numerical analysis on a hydrokinetic energy conversion system which was coupled with a multi-pole permanent magnet generator via Matlab simulation and testing. The study focuses on the electromechanical dynamics of the system. The system, which is being analysed consists of a NECI rotor, a gearbox, a permanent magnet generator, power electronics for conversion of power and a simulated resistive load. Analysis of the test data shows that the turbine starts to rotate when the speed of the fluid is between 1.75 and 1.85 m/s. The study shows that the start-up of the generator can be difficult due to the gearbox torque requirements and cogging torque of the generator. These are extra loads that the rotor must overcome at start-up before energy may be extracted. The study developed suitable mathematical models that can be used to represent the system as the models correlated positively with the experimental data taken from the prototype. The researchers explain that further research into the start-up characteristics of the system needs to be done. Improvement of the rotor frame and further understanding of ducting systems need to be investigated further. It was concluded that the mathematical formulations and the Matlab models have proven to be successful as the results from the models matched the experimental results. He further states that these models can be refined and adjusted for other hydrokinetic systems.

Ikoma et al. (2008), researched the validation of computational fluid dynamic (CFD) models on a three-bladed Darrieus water turbine with the numerical calculations and experimental test data. The research focused on the hydrodynamic forces that act on the turbine-fixed blades at various attack angles and the characteristics of the torque on the blades. These areas of interest are discussed with experimental CFD models. It was concluded by the researchers that the computational analysis was validated by comparison with the experimental test results. The research also includes optimization of the torque performance of the turbine by controlling the attaching angle of the blades if the attack angles do not change. The control theory was done by using the blade element and momentum theory.

Zhang et al. (2012), conducted a study on the hydrodynamic characteristics of a vertical-axis Darrieus turbine. The study combines experimental and numerical simulations. These models are used to test the turbines' kinematics and dynamics under simulated flow conditions. Using the results from the study performance upgrades to the turbine can be implemented. Validation of the CFD simulation results with the corresponding fluid dynamic governing equations which have been used and concluded that this type of turbine has good self-starting capabilities. The performance of the turbine power and structural integrity can be improved by adjusting the range of the limit angle. Zhang et al. further observed that optimizing the attack angles of the turbine blades contributes to increased performance of the turbine along with decreasing the vortex formed by the rotating blades.

Davis (1997), summarizes work that has been conducted in the field of vertical axis water turbines, identifies potential hydro-energy harvesting sites, areas of design for the Davis turbine, project development and financing for the project. The Davis Turbine is based on the Darrieus turbine and hence is a lift-type water turbine. The turbine is housed in a concrete frame which serves as a ducting system. In the study, Davis proposes to use a tidal fence to harness the maximum amount of power from the resource. A tidal fence has a rectangular cross-section that can hold multiple turbines. With the turbines placed above each other, one main rotating shaft can be used to couple all the turbines. The shaft is fixed on the top and bottom of the fence as well as the top and bottom of the turbines to eliminate vibration. The tidal fence also serves as a duct to increase the flow of the tidal resource. For the field testing a variable speed generator was used as the tidal resource flow is not constant.

Yang and Shu (2012) conducted a study on the optimization of hydrofoils which are used for a helical vertical axis turbine for increased performance. The optimization was done by traditional genetic algorithms and a hierarchical computational model. Yang and Shu used a Bezir curve to parameterize the marine current hydrofoil and numerical analysis was conducted to evaluate the performance of the turbine. The lift-to-drag ratio is discussed in detail in the study. Performance and computational tests were conducted to compare the optimized hydrofoil to that of other competitive hydrofoils. The experimental results verify that the optimized hydrofoil is more suited for marine current turbines and also is of benefit to the turbine efficiency and can be seen as a positive prospective hydrofoil for the vertical axis helical turbine.

Niblick (2012) conducted an analytical, computational and experimental analysis of a Gorlov-based helical turbine for the generation of micro-power. The thesis also includes the feasibility of using micro-scale tidal generation to power autonomous oceanographic instrumentation and emphasizes turbine design and performance. The components of the system are reviewed and include the turbine, gearbox, control system, convertor and battery storage bank. Niblick also developed a steady-state model for the tidal resource with a peak current velocity of 1.5 m/s. the testing includes performance characteristics, freewheel stall, static torque as a function of the turbine blade azimuthal angle and performance degradation and inclination angles up to 10^{o} and stream-wise wake velocity profiles. The study also shows how the turbine efficiency increased with an increase in the flume velocity. Modelling of the free-vortex characteristics of the flow was done and modified to simulate the helical turbine performance. The model and analytical results were compared to the experimental results for an array of strut designs and inflow velocities. Niblick concluded that the model results were validated by comparison to the experimental data but deviated under certain conditions and recommends further study of secondary effects for high chord-to-radius ration turbines.

Shino et al. (2002) conducted a study on the output characteristics of a Darrieus water turbine with helical blade profiles. The study was conducted via hydrographical testing of various helical turbines and the results compared to that of the straight blade Darrieus turbine. Shino, et al. concluded that the helical turbines with different inclination angles did not affect the turbines' start characteristics but the solidity of the turbine did. The torque on the turbine and subsequently the efficiency of the turbine increases with an increase in the inclination angle of the turbine blades. The helical turbine, however, was found to be best suited as the helical-bladed turbine has a lower pulsation rate than that of the straight-bladed Darrieus turbine.

Biadgo et al. (2013) recognized that most of the studies that were done on vertical axis wind turbines (VAWTs) were based on the prediction of the efficiency of the device. The research was focused on the progress and developments of aerodynamic models for studying VAWTs with an emphasis on the stream tube model approach. The study investigates a straight-bladed Darrieus turbine by numerical and analytical methods using a NACA 0012 blade profile. The numerical CFD analysis is based on a two-dimensional unsteady flow around the VAWT model by solving the respective Navier-Stokes equations. A comparison of the double multiple stream tube model used for analytical analysis and numerical models was done to validate the mathematical approach used. The results from both models depict negative performance for lower tip speed ratios. Biadgo, et al. concluded that the negative performance at lower tip speeds was due to the inability of the Naca profile to self-start.

Rossetti and Pavesi (2013) researched the different numerical methods used to analyze wind turbine self-start-up characteristics. The analysis of the start-up characteristics of a turbine is of importance as this allows one to design and obtain a turbine that would require much less effort to extract energy from the flow medium. In the study, the blade element momentum model was compared with a three-dimensional CFD model. Results of tip speed ratio versus power coefficient and the development of thrust coefficient highlighted the strengths and limitations of each of the mathematical predictions. The study compares the difference in 3D and 2D approaches in CFD analysis and further explains how 3D simulations, although more computationally expensive, show tip effects that have a positive influence on the start-up of the turbine by increasing the torque coefficient for a tip speed of 1.

3 Performance characteristics of a helical crossflow turbine

To evaluate a turbine system, one first needs to understand the parameters that govern the turbine. These associated parameters directly influence the power output and efficiency of the turbine. The following section of this paper describes the many parameters of a helical crossflow turbine.

The starting torque of the turbine is a key characteristic of any turbine. The starting torque indicates the force that is needed to initialize the rotation of the turbine. The starting torque is due to the turbine weight and other components which may be coupled to the turbine. This torque needs to be overcome for the turbine to start rotating. Once the starting torque is overcome, the torque of the turbine is calculated by using the relevant lift and drag coefficients for the airfoil profiles which are used for the turbine to work out the normal and tangential force which act on the center of pressure of each turbine blade. The averaged torque for the turbine is used to work out the torque coefficient of the turbine which is depicted in the following equation:

$$C_Q = \frac{\mathrm{T}}{0.5\rho U_\infty^2 R A_c} \tag{1}$$

e torque coefficient in conjunction with the turbine's tip speed ratio is the value that is used to calculate the performance of the turbine. Generally, the turbine's performance coefficient is taken as the measure of the turbine's efficiency. The efficiency of the turbine is the amount of mechanical work generated from the incoming flow.

Tip speed ratio is one of the key performance monitoring aspects needed for any hydrokinetic turbine or wind turbine. The tip speed ratio is the ratio of the speed at the tip of the blade to that of the incoming fluid medium. It can be seen that this value is indirectly proportional to the free stream velocity from the following governing equation:

$$\lambda = \frac{\mathrm{R}\omega}{\mathrm{U}_\infty} \tag{2}$$

The angle of attack was determined by incorporating a relationship between the resultant velocity and the tip speed ratio of the turbine. This method of determining the angle of attack allows one to fully understand the theoretical attack angle of the blade through one full revolution of the blade. The angle of attack (α) is calculated as follows:

$$\alpha = \frac{sin\theta}{cos\theta + \lambda} \tag{3}$$

A single-blade analysis was conducted to understand the angle of attack as the blade moves through the revolution of the turbine. Figure 3-1 illustrates how the range of the angle of attack decreases as the tip speed ratio increases. The red line indicates a tip speed of 2.5 and the blue a tip speed of 2. This does not mean that at very high tip-speed ratios the turbine will perform more efficiently. The proposed turbine has an optimum tip speed which was obtained using the double multiple stream tube mathematical model. This model was confirmed with experimentally obtained results from Lazauskas and Kirke (2012).

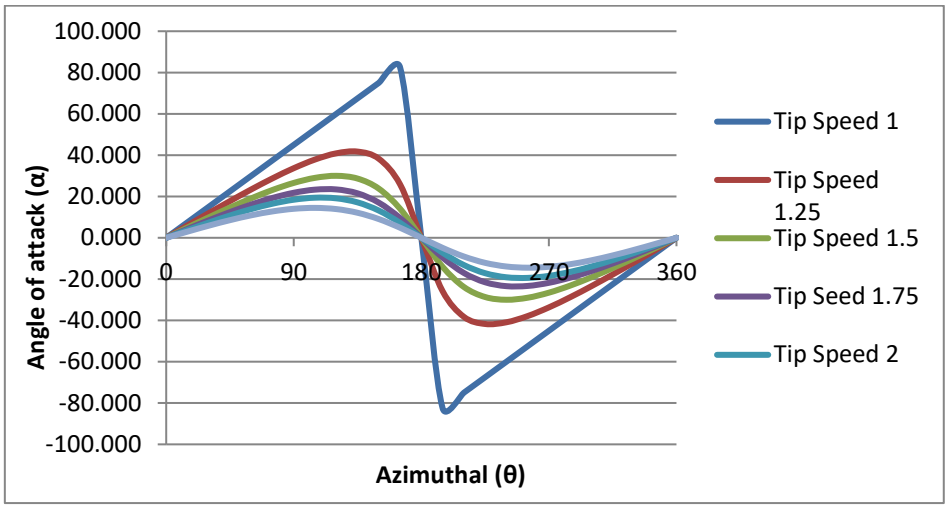

Figure 3-1: Angle of Attack Vs. Azimuthal Angle

When the torque produced by the turbine is known, the amount of power that can be extracted from the turbine shaft may also be calculated using the power coefficient (C_p). The power coefficient is the ratio of extracted power from the turbine to the theoretical power of the fluid resource. The unitless value can also be directly related to the torque coefficient and tip speed ratio. The power coefficient may also be viewed as the turbine's efficiency.

$$C_p = \frac{\mathrm{T}\omega}{0.5\rho \mathrm{U}_\infty^3 A_c} = C_Q \lambda \tag{4}$$

The performance of the turbine is the ultimate goal of the turbine monitoring. The performance coefficient determines the amount of energy the turbine can extract from the incoming flow. According to the Betz limit the maximum amount of energy for any reaction turbine using a renewable source of flow medium to extract is 59%. For a Darrieus-based turbine with a Gorlov helical profile the maximum power coefficient of 35 – 40% and a kinetic flow to mechanical energy efficiency of 90%.

Research conducted by Fiedler and Tullis (2009) found that a toe-out blade pitch configuration advantages the performance of the turbine compared to that of a toe-in blade pitch configuration. Fiedler and Tullis also found that the most optimum toe-out angle was between 3° and 8°. The angle of attack changes incorporating the pitch angle of the blade (β) is calculated as follows:

$$\alpha = \frac{sin\theta}{cos\theta + \lambda} - \beta \tag{5}$$

The crossflow turbine chosen was to exploit the lift force generated by the fluid flow on the turbine blades. The blades, however, do still experience drag as they rotate. The lift (C_L) and drag (C_D) coefficients are directly related to the lift and drag force for the given blade geometric profile. The coefficients of lift and drag were obtained from Sheldahl and Klimas (1981) as this provided various lift and drag coefficients for various Reynolds numbers. The lift and drag coefficients are respectively given as follows:

$$\mathrm{C}_L = \frac{L}{0.5\ \rho \mathrm{U}_{rel}^2 cH} \tag{6}$$

$$\mathrm{C}_D = \frac{D}{0.5\ \rho \mathrm{U}_{rel}^2 cH} \tag{7}$$

Applying Equations 6 and 7 to different azimuthal positions of the blade provides a very basic understanding of the forces generated by the flow but this does not give an accurate depiction of the flow behavior within the

vicinity of the turbine. The resultant of these forces generates torque on the turbine shaft which is used to drive the coupled generator. This forms the basis for obtaining the torque coefficient (C_Q) of equation 1.

$$T = R(L\cos\alpha - D\sin\alpha) \tag{8}$$

The tangential force is directed towards the positive leading edge of the profile and the normal force is directed inward, towards the center of rotation of the turbine. However, the tangential and normal forces may be difficult to obtain, so a relationship between the lift and drag coefficients and the relative angle of attack at the "1/4 chord" was used to obtain the tangential and normal coefficients. The tangential and normal force coefficients may be calculated by the following equations respectively:

$$C_N = C_L\cos(\alpha) + C_D\sin(\alpha) \tag{9}$$

$$C_T = C_L\sin(\alpha) - C_D\cos(\alpha) \tag{10}$$

Figure 3-2 depicts the tangential and normal force vectors about the lift and drag force vectors that impact the blade profile. From this, we may conclude how the turbine exploits the lift force generated by the hydrofoil. Figure 3-2 also shows a pitched blade profile and the component vectors induce turbine rotation.

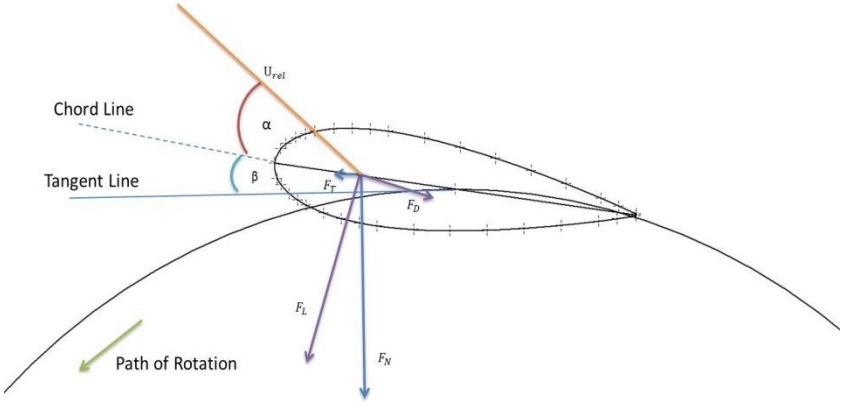

Figure 3-2: Normal and Tangential forces on blade profile

4 Numerical Modelling of the turbine

The turbine which was designed was proposed to be mathematically modelled using the double multiple stream tube theory. This was conducted to understand the performance characteristics of an ideal situation. The following section covers the numerical modelling of the approach adopted form Biadgo et al. (2013) which can be seen in the Figure 4-5.

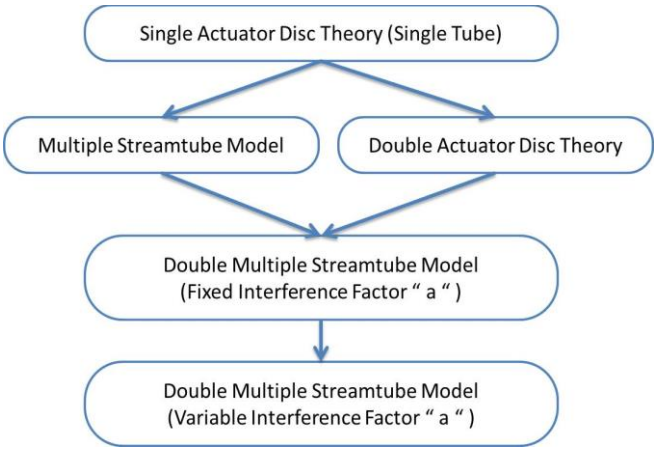

Figure 4-1: Double actuator disc theory expansion, Biadgo et al. (2013)

4.1 Ideal actuator disc theory

The actuator disc theory serves as the basis for multiple stream tube theory. This theory is built on the foundations of propeller theory but enhanced by breaking the conventional predicted stream path into multiple stream tubes which are used to analyse the blade at different positions in its rotation.

Figure 4-2 illustrates the actuator disc control volume conceptualized mathematically by Rankine and Architects (1865). This is known as an ideal actuator disc model and the flow conditions are taken as steady and incompressible. The concept of using an actuator disc and governing control volume was first proposed by Rankine and thus built on throughout the decades by various other mathematicians and scientists such as Froude (1889).

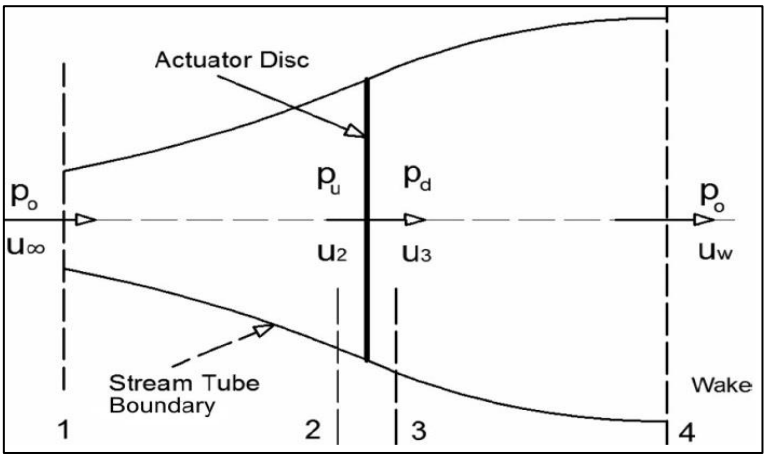

Figure 4-2: Single Actuator Disc Theory, Biadgo et al. (2013)

For the given case, the velocity just after the rotor is of concern. The theory states that since the turbine is extracting energy from the flow, the velocity at the outlet should be less than the inlet by some factor. This factor is known as the axial induction factor and is understood as the fractional decrease of free stream velocity to that of the velocity at the rotor disc. The theory indicates that there is a steady decrease in flow velocity within the control volume from inlet to outlet. The theory also depicts a drop in pressure across the actuator disc showing that the turbine is extracting energy from the flow, (Figure 4-3).

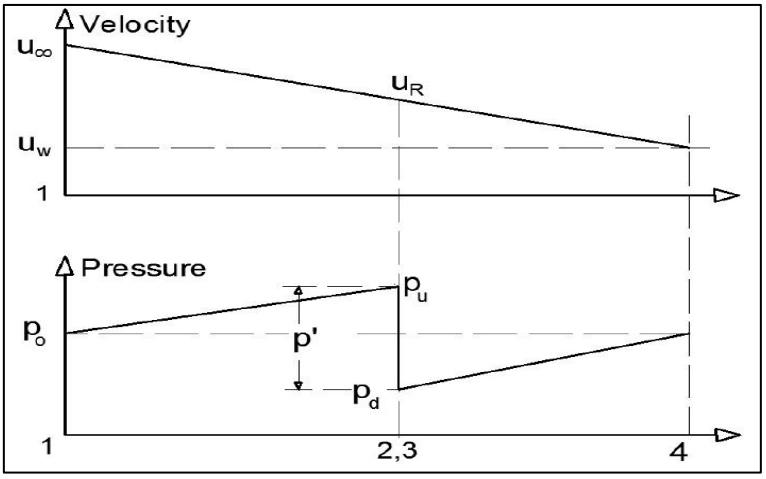

Figure 4-3: Velocity and Pressure characteristics for Actuator disc theory, Biadgo et al. (2013)

To understand how the fluid interacts with the turbine blades, one needs to understand the vectors that are created from the fluid interaction with the turbine blades. Figure 4-4 illustrates the turbine's blade velocity vectors. These angles and vectors change as the turbine rotates at different speeds. The helical crossflow turbine

exploits the lift generated by the hydrofoil profiles, the same as the airfoils, to obtain rotation. Due to the turbine being vertical axis in orientation, the direction of the flow is irrelevant as long as the flow is somewhat perpendicular when entering the turbine.

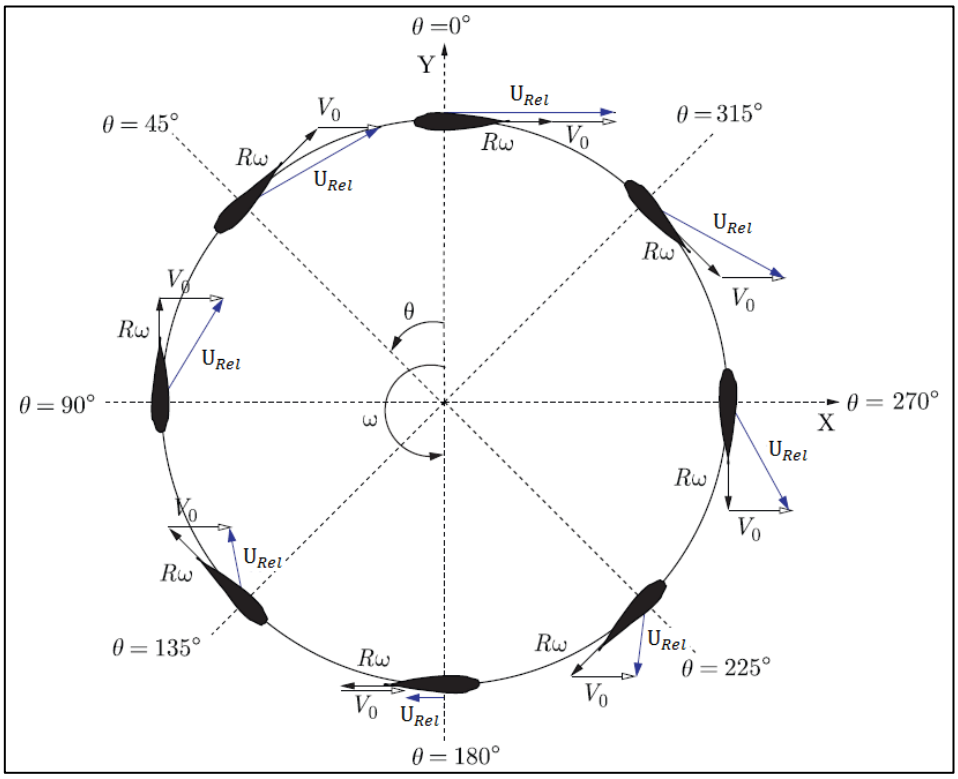

Figure 4-4: Blade velocity vectors through Azimuthal angle change, Antheaume et al. (2008)

The multiple stream tube models are implemented by discretizing the turbine rotational field into multiple stream tubes. This method of analysis only takes into account the upstream characteristics of the flow. This does not separate the upstream and downstream as more vortices are formed downstream due to blade interaction during rotation. These vortices which are created by the upstream section propagate down the turbine and cause interference with the shaft and downstream blades. This directly affects the performance of the turbine negatively.

4.2 Double Actuator Disc Theory

On closer examination of the double actuator disc theory (Figure 4-5), it can be graphically seen how the free-stream velocity changes through interaction with the blades and creates induced velocities. Figure 4 5 illustrates a multiple actuator disc theory, by Biadgo et al. (2013).

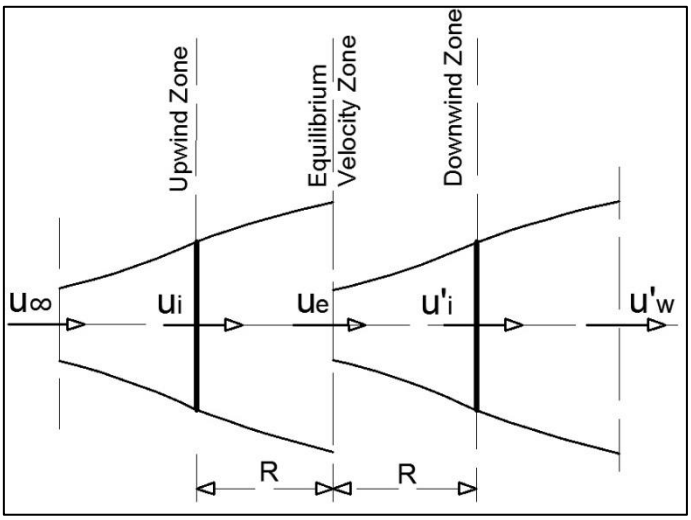

Figure 4-5: Multiple Actuator Disc Theory, Biadgo et al. (2013)

The induced velocities for the upwind and downwind sections are illustrated in equations 4 and 5 respectively. It can be concluded that the induced velocity of the downwind actuator is dependent on the exit velocity of the upwind actuator. These equations provide the basis for the calculation of the relative velocity of the fluid flow and the constantly changing attack angles of the turbine blades, by using the interference factors which are obtained via an iterative method.

$$u_i = (1 - a)U_\infty \tag{11}$$

$$u_i' = (1 - a')(1 - 2a)U_\infty \tag{12}$$

Equations 4 and 5 take into account the induction factors which are the losses encored through the turbine system due to the extraction of energy. In the downwind section of the turbine, there exist two induction factors that are being considered. This is due to the already decreased velocity from the upwind section and further reduction due to downstream blade interaction.

4.3 Multiple Stream Tube Theory

The multiple stream tube model is implemented by discretizing the turbine rotational field into multiple stream tubes. This method of analysis takes into account the entire control volume. The model was developed by Strickland (1975) and is based on the initial momentum theory by Rankine and Architects (1865). The improvement of this model compared to that of the single tube theory is that the concept of discretizing the control volume adds new induced velocities allowing for more accurate analyses of the turbine through the turbine's rotation. As each stream tube has its velocity, the accuracy of this numerical prediction is dependent on the number of stream tubes incorporated. Figure 4-6 illustrates the discretization of the turbine based on the multiple stream tube approach.

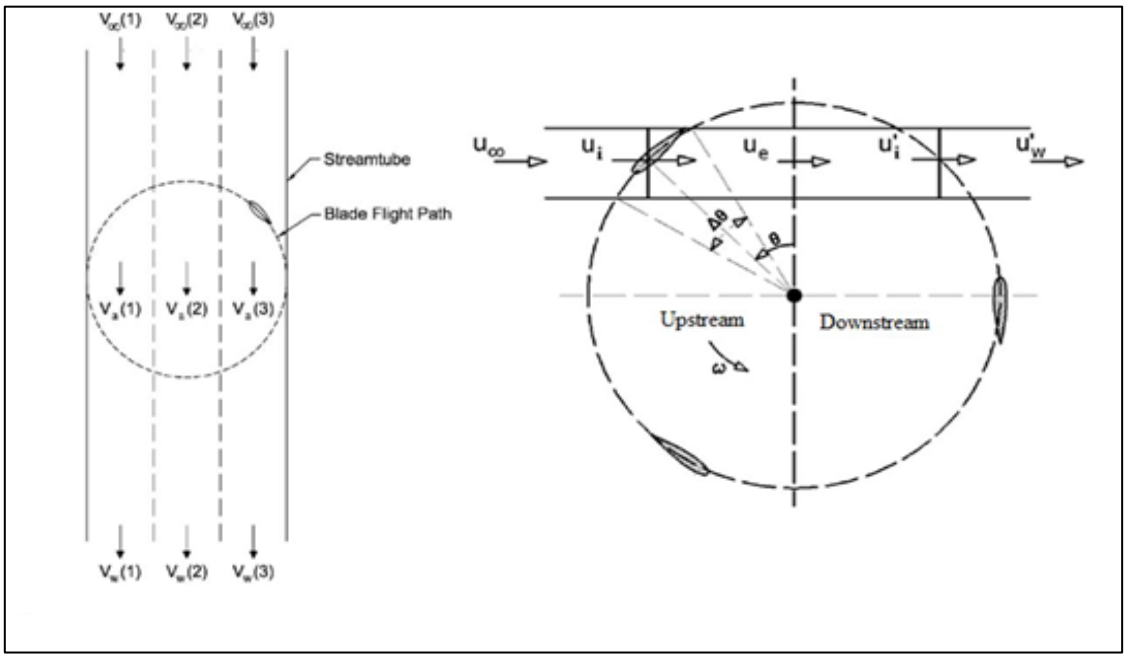

Figure 4-6: Double Multiple Streamtube Model, Paraschivoiu and Delclaux (1983), Biadgo et al. (2013)

This model does not separate the upstream and downstream as the double actuator disc theory does. The vortices which are created by the upstream section propagate down the turbine and cause interference with the shaft and downstream blades. This directly affects the performance of the turbine in a negative respect.

By combining both the multiple stream tube model and the double actuator disc theory, a more accurate numerical model was developed. This model has the benefits of both approaches and considers the necessary physics which needs to be accounted for, however, wake interference is not included due to its complexity.

4.4 Double Multiple Stream Tube Theory (DMST)

The double multiple stream tube model solves the equations allocated for the upwind and downwind sections simultaneously. The equations are linked to the stream-wise force at each actuator disc. The following equations are obtained from the conservation of momentum and the aerodynamic coefficient characteristics of the turbine blade profiles being implemented. The equations for the upwind sections of the turbine, including the attack angle, are as follows:

$$w = \sqrt{(u_i \sin\theta)^2 + (u_i \cos\theta + \omega R)^2} \tag{13}$$

$$\alpha = \tan^{-1}\left(\frac{(1-a)sin\theta}{(1-a)cos\theta+\lambda}\right) \tag{14}$$

It can be seen by these equations that the induction factors are taken into account within the angle of attack of the blade with the DMST approach. The following set of equations depicts how the downwind of the turbine was calculated. Since the DMST incorporates the sectioning of the turbine's control volume into two sections, there now exist two sets of induction factors. The inclusion of this means that the relative velocity and attack angle of the turbine has to be calculated for both upwind and downwind separately.

$$w' = \sqrt{(u_i' \sin\theta)^2 + (u_i' \cos\theta + \omega R)^2} \tag{15}$$

$$\alpha' = \tan^{-1}\left(\frac{(1-a')sin\theta}{(1-a')cos\theta+\lambda}\right) \tag{16}$$

5 Excel Numerical Model

To correctly use these equations within an iterative solver, there needs to be a common value to compare to the analytical data. By reverting to the multiple stream tube model and the hydrodynamics of the turbine various new equations can be resolved using the multiple stream tube approach.

The tangential (C_t) and normal (C_n) coefficients of the turbine are highly important in the calculation of the performance of the turbine. As the multiple streamtube model analyses the turbine performance for one full revolution from 0° to 360°, the previously stated coefficient methods cannot be directly incorporated into the model, hence a relationship with the constantly changing attack angle (α) needs to be established. Equations 9 and 10 with the use of the new attack angles can be solved to accurately obtain the normal and tangential coefficients for the blade profile.

The common variable between the analytical equations and the numerical models was the thrust coefficient. The accuracy of the double multiple stream tube model is directly dependent on the total number of discrete stream tubes being used. The momentum balances for each of the stream tubes are calculated individually. The separate calculations result in the model having to acquire the "*N*" amount of induction factors for each stream tube. The induction factor for each stream tube will be different due to the blade attack angle and resulting relative velocity being different in each stream tube. Referring to Figure 4-6, the average aerodynamic thrust on a turbine, with a "*B*" number of blades can be expressed by Equation 17. Equation 17 was derived on the basis that each of the turbine blades spends $\Delta\theta/\pi$ percent of the rotational time in the stream tube.

$$T_{avg} = 2\left(\frac{B\Delta\theta}{\pi}\, T_i\right) \tag{17}$$

Taking into consideration that the stream tube has a wetted swept area of $A=hR\Delta\theta sin\theta$, like the torque coefficient of the entire turbine, the non-dimensional thrust coefficient of the turbine may be derived, as seen in equation 18.

$$C_{Thrust} = \left(\frac{Bc}{2R}\right)\left(\frac{w}{U_\infty}\right)^2 \frac{2}{\pi} C_t \left(\frac{\cos\theta}{\sin\theta} - C_n\right) \tag{18}$$

Within the numerical model the average torque on a rotor with, "*B*" number of blades, in one complete turbine revolution and blade length "*h*" is given by equation 19.

$$Q_{avg} = B \sum_{i=1}^{N_\theta} \frac{Q_i}{N_\theta} \tag{19}$$

The corresponding torque coefficient can be derived from the average torque and is shown in equation 20.

$$C_Q = \left(\frac{Bc}{2R}\right) \sum_{i=1}^{N_\theta} \frac{\left(\frac{w}{U_\infty}\right)^2 C_t}{N_\theta} \tag{20}$$

The Excel numerical model uses the known relationship of tip speed ratio and torque coefficient to obtain the performance coefficient of the turbine and is given by equation 21.

$$C_P = \lambda C_Q \tag{21}$$

The equations which were discussed at the beginning of this section were adapted and implemented in Microsoft Excel. This was done using Excel Macros which were built especially to calculate the turbine performance based on its coefficients of lift and drag as well as the corresponding tangential and normal coefficients for various attack angles. Figure 5-1 shows the basic methodology logic behind the programming based on the research conducted by Biadgo et al. (2013)

The coefficients of lift and drag were generated within an external program, which is used widely for the generation of lift and drag coefficients, called Xfoil. The generated lift and drag coefficient values were used via a lookup table function in Excel and implemented in the various equations explained above. The analysis was

conducted on two types of turbines to validate the theory of using a fixed-pitch turbine within a limit of 0° to 8° as stated in Chapter 7. The most suitable blade profile was chosen to be the NACA 0024 profile.

The analysis was conducted for tip speed ratios from 1 to 2.5 in increments of 0.25. This range was chosen based on previous literature performance on similar turbine designs. For the angle of attack for each tip speed, an increment of 30° was initially chosen and then reduced to 7.5° to refine the performance curve. Within the Macros code a Glauret empirical formula was imbedded to calculate the thrust coefficient from the analytical equation for $0.4 < a < 1$, as this is not always possible for an induction factor of 0.5.

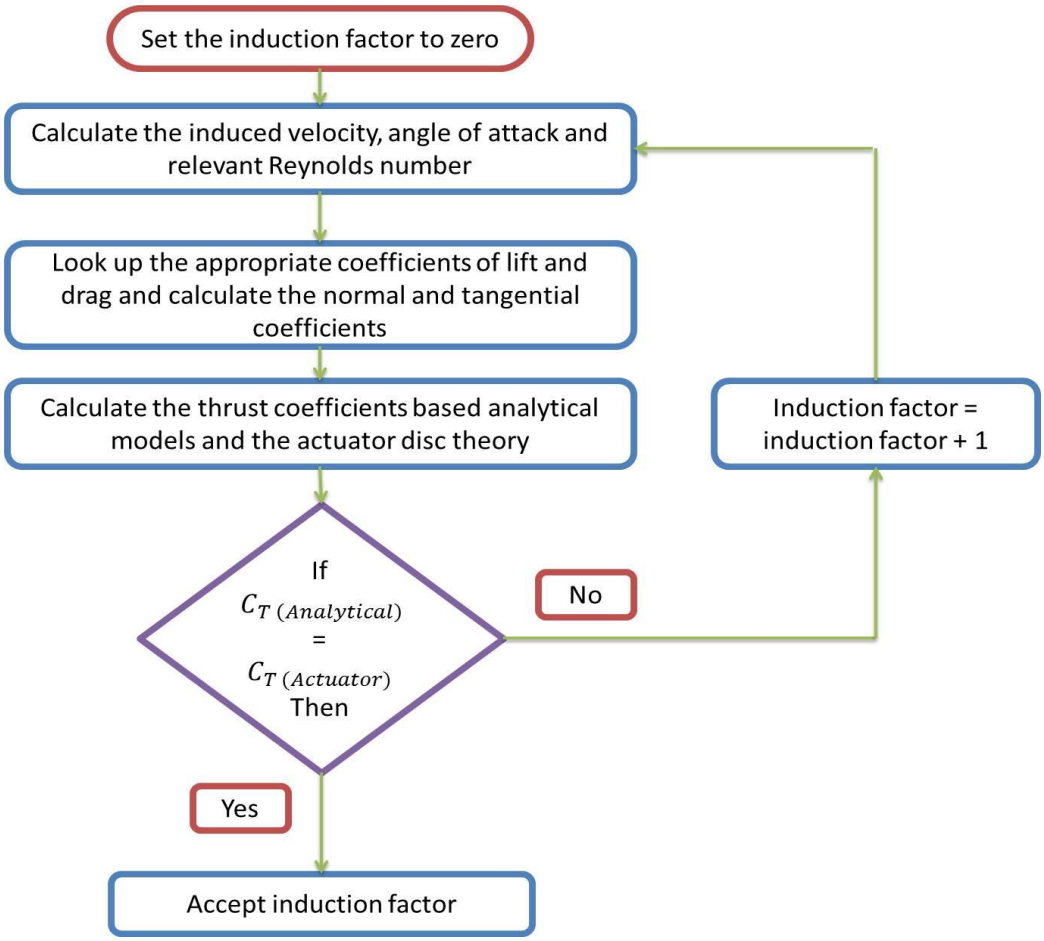

Figure 5-1: Flow Diagram of Program Logic, Biadgo et al. (2013)

Within this iterative solver, vortex modelling of the turbine was not included which may lead to somewhat of an inaccurate result, but the effects may be taken as minimal. The vortex modelling of the system was omitted due to the complexity of the model which could not be adequately coded within Microsoft Excel. This type of model can be obtained via external programs such as SANDIA Labs CACTUS modelling program as stated by Niblick (2012).

6 Qblade Model

QBlade is a freeware modelling tool that is based on the original Xfoil coefficient generator. Xlrf5 was developed after Xfoil to enhance the user-friendliness of the program. With the increase of developing wind turbines and the ongoing research into optimizing them, there became a need for a suitable renewable energy turbine performance tool. As these turbines made use of various air foil profiles and required lift and drag coefficients, QBlade was developed from Xflr5 by Marten et al. (2013) in conjunction with TU Berlin. This new tool allowed for blade design to be conducted within the program by selecting the relevant blade airfoil profile. Once the profiles for the blade sections are chosen, the Xfoil embedded program is used to generate lift and drag

plots for each of the air foil profiles. Polar plots are extrapolated from these plots to produce approximated lift and drag coefficients for one entire 360° revolution. Unlike the Xflr5 program, the QBlade program has the addition of a built-in double multiple stream tube solver which can incorporate tip loss and variable induction factors.

Figure 6-1 illustrates the selection of the Naca 0024 blade profile and the original Xfoil discretization of the profile was selected to its maximum limit of 200 panels, which is the highest resolution that can be chosen by the program.

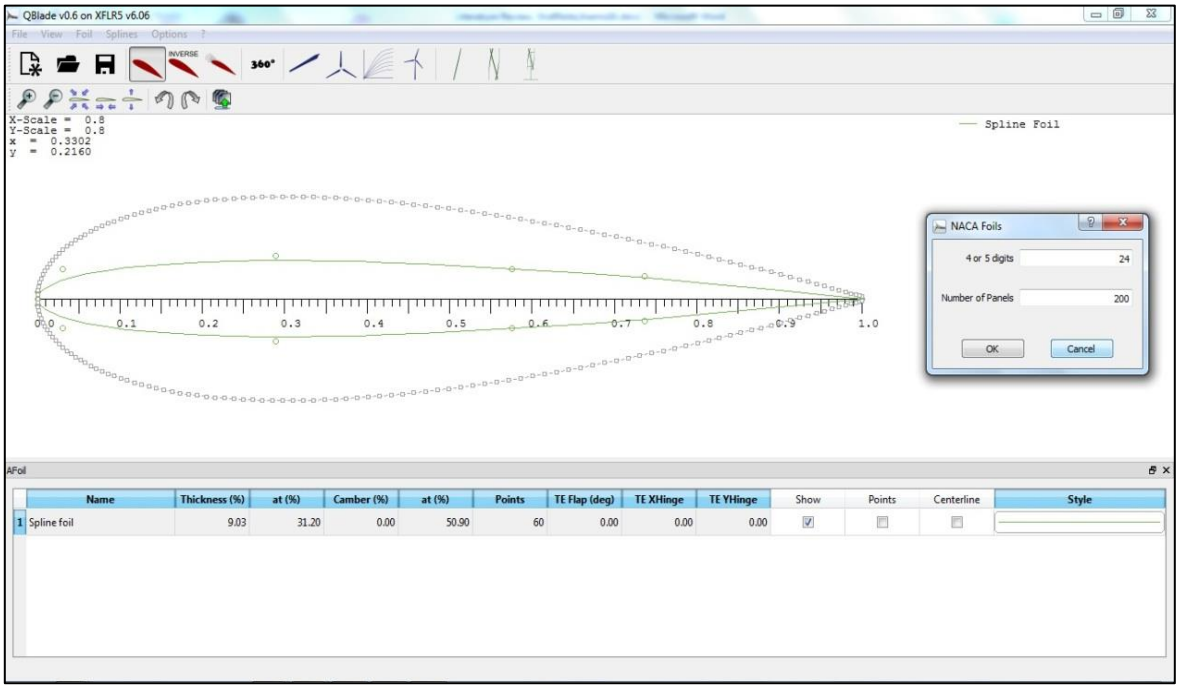

Figure 6-1: Selection of blade Airfoil/Hydrofoil Profile

The second stage of the analysis was to accurately define the analysis of the blade profile by setting relevant parameters. The parameters were defined for the surrounding fluid medium, surrounding environment, blade characteristics and the testing conditions. The chord length was set to 0.02m with the chosen 20.01 mm chord length and the blade mass was taken as 50 grams as the chosen material for the blade taken to be ABS plastic. The surrounding fluid medium was taken to be water and the density and dynamic viscosity were chosen appropriately. The density of water was taken to be 1000 kg/m^3 and the kinematic viscosity of water was taken to be 1.004x10^{-6} m^2/s on an assumption that the water is at 20°C. The surrounding environment characteristic is dependent on the NCrit value of the analysis. This value determines the cleanliness of the testing environment scaling from 1 to 12 where 1 is taken as the most unclean and 12 as the cleanest. In terms of cleanliness, the NCrit numbers depict a user assumption of the number of environmental debris that exists. For the analysis, an NCrit value of 10 was chosen to depict a moderate amount of cleanliness in the test.

To determine the amount of energy extracted from the flow, a range of Reynolds numbers was selected within a multi-thread analysis using the above information and undergoing the iterative calculations for each Reynolds number. Before the solver can solve the relevant calculations regarding Navier-Stokes and continuity equations, the angle of attack range and increments must be set in the XDirect panel shown in Figure 6-2. The range was defined to be from -10° to 10° with an increment of 0.1°. This was done to enhance the refinement of the calculations for each attack angle as larger increments may sometimes not take into account certain flow characteristics.

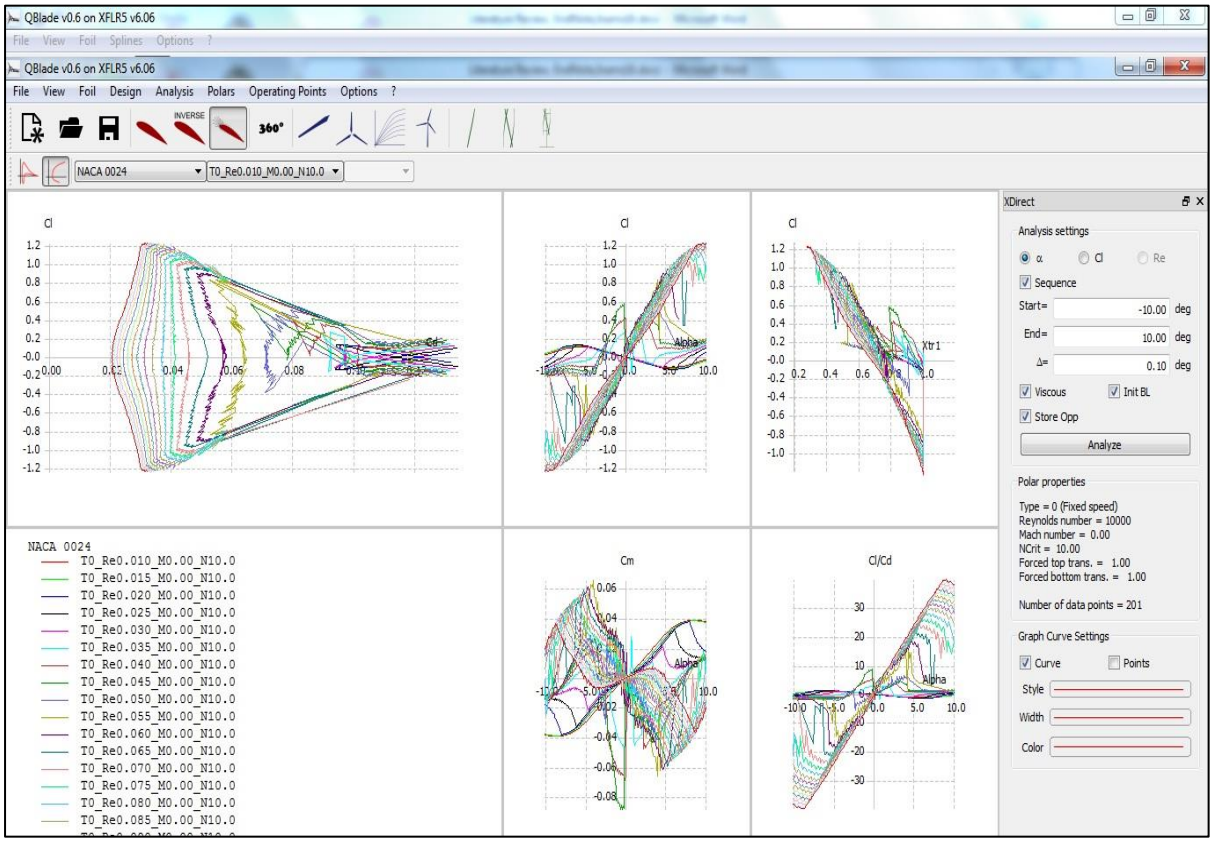

Figure 6-2: Multi-thread analysis for the Naca profile

The next step in the process of analysis is to create a polar plot of the attack lift and drag coefficients for the full revolution as the attack angles are constantly changing. Lift and drag coefficients are taken for the entire 360° of the revolution but it must be noted that the angles of attack of the turbine blades do not reach over 75°. The maximum amount the attack angle will reach through a turbine revolution is 75° – 85°. The attack angle is subject to the tip speed ratio of the turbine as stated in equation 3 explicitly and equations 14 and 16 with regards to the double multiple stream tube model. This identity of attack angle change is accounted for in the code of the program.

The polar plots in the QBlade program can be obtained via two methods. The first method of obtaining the polar plot is the Montgomery extrapolation technique and the second it the Viterna-Corrigan post-stall model technique. The Montgomery extrapolation assumes that the flow around the blade can be treated as a potential flow from 0° to 180° of the profile's attack angle. The extrapolation estimates the flow behavior is approximated to that of a stalled thin plate used for the airfoiled. A blending function is then incorporated into the profile at transition points along the profile for the potential flow curve ling and the flat plate curve. The Viterna-Corrigan post-stall model utilizes empirical equations for the analysis. The model exhibits an ideal case and thus results in approximately constant power output after a stall on the profile. This model depends on the aspect ratio (*AR*) of the turbine. For blades that have various aspect ratios, new polar plots need to be generated for the given section.

With the analysis of the vertical axis helical turbine within this study, both of these models were used as the aspect ratio needed to be specified and the non-ideal case of extrapolation needed to be conducted for the turbine. A Reynolds number of 100 000 was used for the polar plot and analysis as this results in a flow velocity of 0.6 m/s which is close to the estimated start-up velocity of the turbine. Figure 6-3 shows the comparison of both polar plots using Montgomery extrapolation with a fixed aspect ratio and a Viterna-Corrigan post-stall analysis. The red line defines the Viterna-Corrigan method and the green line represents the Montgomery method, both using an aspect ratio of 3. By considering simulated stall behavior at relevant transition regions

along the blade, the Montgomery method shows a more realistic curve compared to that of the Viterna curve, as the Viterna curve shows a constant change in the lift and drag coefficients for the entire polar which is known not to be true due to stall occurrences.

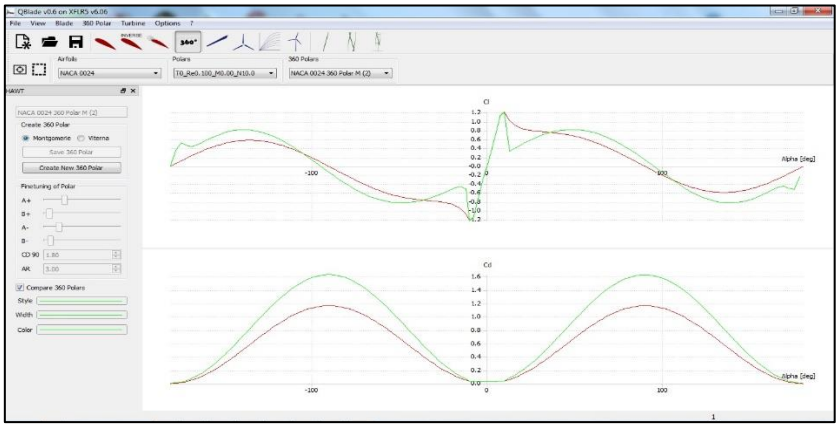

Figure 6-3: Polar plots suing both extrapolation methods

The polar plot chosen was the Montgomery extrapolation with a specified aspect ratio. From this, the blade was designed in the program by assigning each blade section to the chosen polar plot. This is done so that when the double multiple stream tube model is run, the coefficients of lift and drag are incorporated accordingly. The turbine radius, blade height, angle of twist and inclination angle are defined and there is an option to optimize the blade design regarding the chosen turbine. Figure 6-4 shows the blade design parameters on the right and the left shows the designed blade. The blade was sectioned into 11 parts, each having a height of 0.01165 m, built on each other, and then optimized to create a helical blade profile with an angle of twist of 91.4°. The sections are necessary for the implementation of the blade element model (BEM) theory. The sections also further discretize the blades so that the multiple stream tube theory may be even more refined in conjunction with the multiple stream tube discretization.

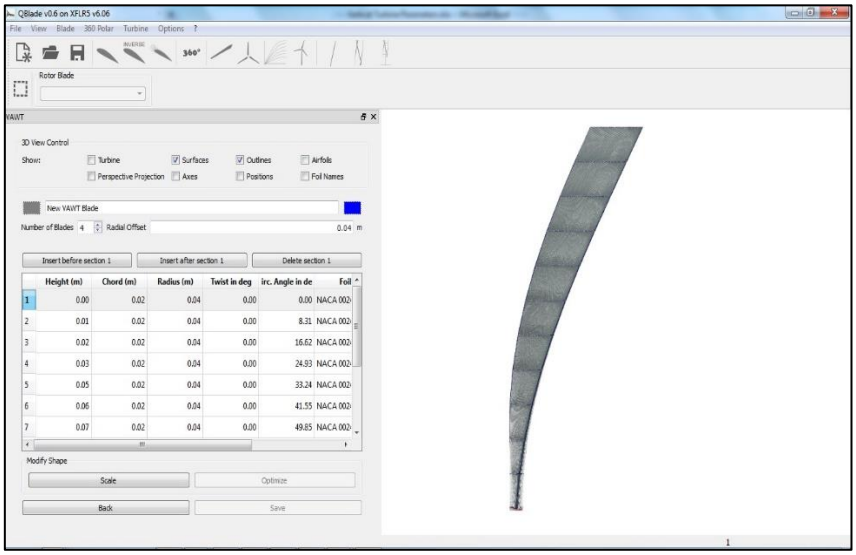

Figure 6-4: Blade design within QBlade

7 Computational Model (CFD)

This section of the paper illustrates the computational methods that were used to analyses the turbine based on the assumed environmental parameters. Star CCM+ was the program that was used to conduct the analysis.

7.1 Geometry modelling

To conduct this analysis, the turbine was first modelled in CAD software and exported to the CFD world as a Stereo Lithography (.STL) file at a high resolution. The ducting system which was also used for the analysis of the turbine was first modelled, incorporated with the turbine model, and exported as a high-resolution file to the CFD program.

7.2 Boundary Conditions

The boundary conditions were captured in the CFD program. These conditions are of utmost importance as they stipulate under what conditions the turbine is subjected to in terms of fluid medium and flow speed as well as pressure within the control volume.

For the following analysis water was chosen with a density of approximately 1025 KG/m^3 to simulate sea water and an assumed flow speed of 0.6 m/s to 1.2 m/s was chosen, in increments of 0.2 m/s for each simulation. This was done to understand how the turbine would perform under various simulated flow conditions. There was no boundary condition added to the ducting system directly to understand how the ducting system would change pressure and flow conditions under standard assumed conditions.

7.3 Discretization of turbine

As a result of the imported, high-resolution STL file, the discretion of the model was made somewhat simpler as a well-defined basic mesh structure already exists for the program to work with. The discretization of the model within the CFD software is called meshing. Meshing breaks down the model into small segments which is used to conduct the standard continuity, Navier-Stokes as well as momentum calculations. The calculations are conducted at each “node” point located at the extremities of the segments within the mesh structure. Many different meshing types could have been utilized for this discretization, but a standard tetrahedral mesh was chosen due to its simplicity. This type of meshing also was not very computationally expensive.

A two-dimensional model was generated from the three-dimensional model due to the ease of processing and low computational requirements. This type of model is proven by Ikoma et al. (2008) and Li et al. (2013) to be a valid way of analysing the turbine. Figure 7-1 depicts the two-dimensional mesh structure of the turbine which is analogous to Figure 4-4.

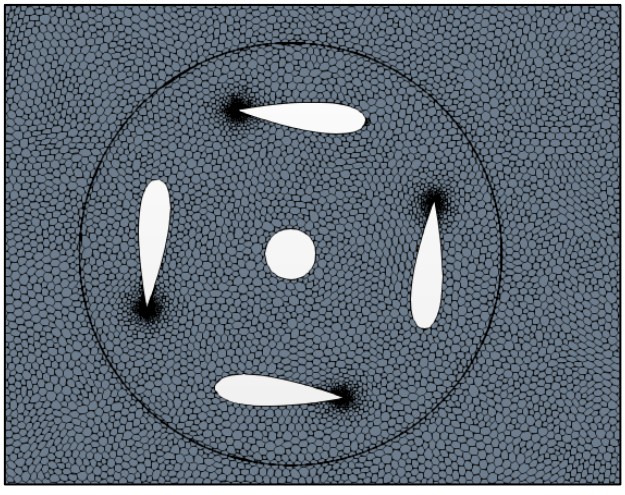

Figure 7-1: Mesh Structure of turbine cross-section.

The model does not depict relative boundary layers but due to the density of the mesh around the airfoil, the mesh was found to be more than adequate to consider the boundary layer effects of the turbine blades.

7.4 Solver Type

The solver which was chosen was an implicit unsteady solver as this type of solver was the closest way of simulating the turbine. The solver makes use of discrete time steps which is in direct relation to the rotating speed (RPM) of the turbine. The solver iterates the various numerical calculations throughout each node point for each time step based on the best-suited number of iterations chosen for the system.

The selection of the number of iterative steps was based on a trial-and-error approach using the two-dimensional mesh model to reduce the duration of the simulation. A time-step monitor was initiated for various iterative numbers. The closest number to reach convergence was chosen. Convergence stated that the system reached a state that had minimum error to that of the previously calculated numerical values. Convergence of the residuals as well as other monitoring systems were also checked to validate this conclusion and obtain reasonable results.

8 Results

The following section illustrates the various results that were obtained from the different methodologies and techniques used to analyses the helical crossflow turbine. For the Numerical model, which was constructed within Microsoft Excel, the main challenge which was encountered was the Glauert empirical condition which needs to be used to account for the variable induction factors that occur in the multiple stream tubes. The iterative solution could not be conducted for the high-resolution simulations but rather for a medium to low iterative solution. Figure 8-1 depicts the performance curves for the turbine at various speeds of incoming fluid. The simulation does not include the ducting system as the velocity speed could not be safely assumed at the time.

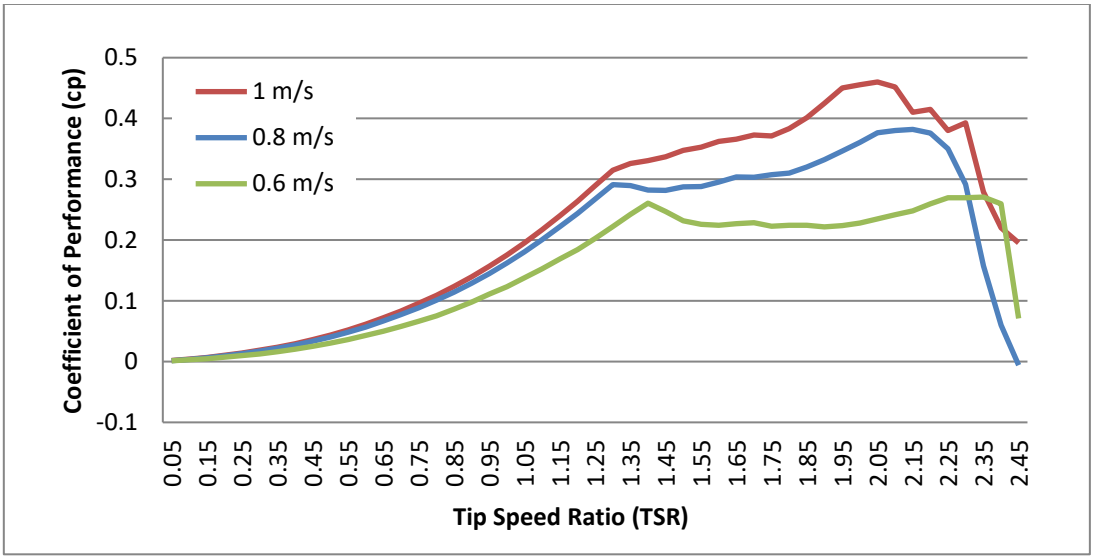

Figure 8-1: Excel Simulation Performance Results

Figure 8-2 depicts the Qblade simulation results for the same simulation conditions that were assumed within the Excel Model. The similarities are clear and it can be seen that the ducting does prove a positive addiction as the performance of the turbine is increased substantially. It should be noted that the ducting system was incorporated with the incoming velocity of 0.8 m/s. It is assumed that ducting optimization to increase the flow slightly would help increase the turbine's performance and power output.

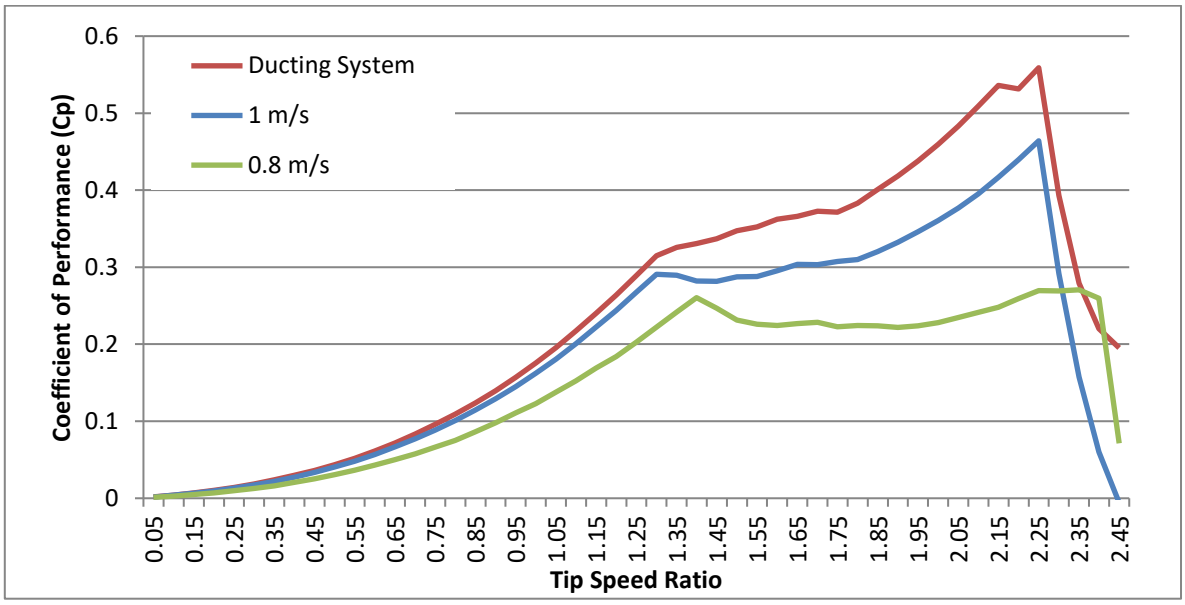

Figure 8-2: QBlade Performance Results

Figure 8-3 depicts the results which were obtained from the CFD analysis including the ducting system. The results were based on obtaining the force on a single blade profile and used in conjunction with the torque equations stated previously, to obtain the coefficient of performance for the turbine system.

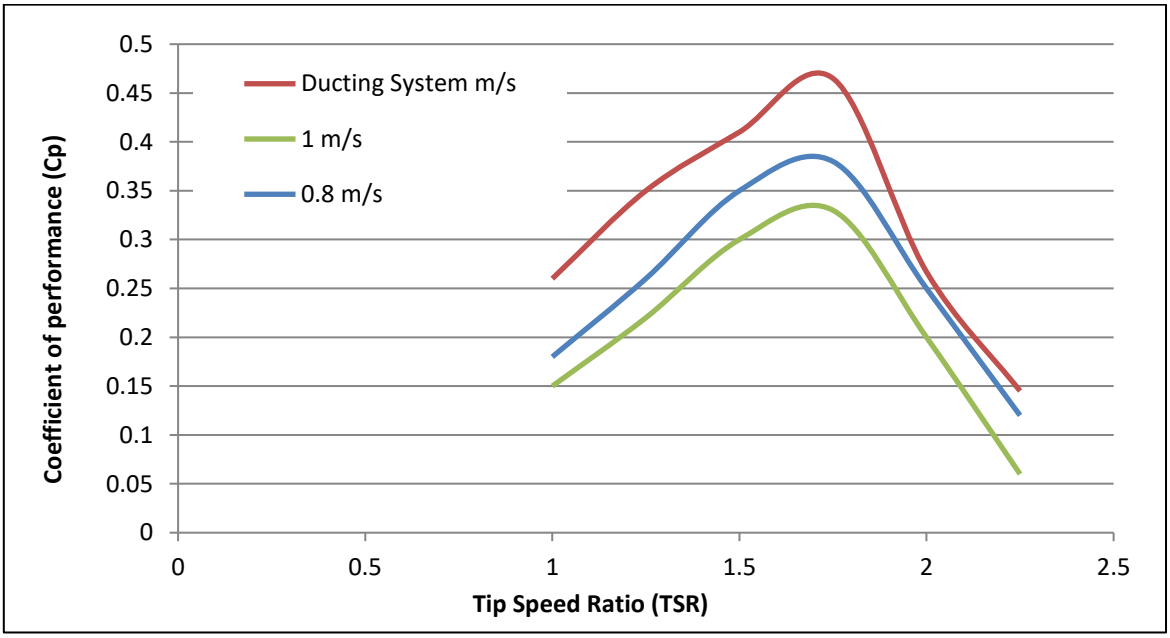

Figure 8-3: CFD Performance Results

Discrepancies in the CFD results can be since the CFD analysis does consider vortex modelling. The solver that was used also considers the recirculation of the wake which is formed by the turbine blade's interaction down-wind section of the turbine control volume. The recirculating, unsteady, turbulent vortices adversely affect the performance of the turbine.

9 Conclusion

The project sought to analyse the helical crossflow turbine by various numerical and analytical methods to understand the performance of the turbine under various fluid velocity speeds as well as with the addition of a

ducting system. It can be seen from the obtained results that each of the analysis which was chosen is highly similar in output to each other. This proves that each analysis was conducted correctly and can now be used as a referencing tool against the testing of the turbine which is scheduled to be conducted in the coming months.

The results obtained in this work demonstrate that the CFD model can effectively predict the hydrodynamic performance of crossflow water turbines.

References

[1] Antheaume, S., Maître, T. & Achard, J.-L. 2008. Hydraulic Darrieus turbines efficiency for free fluid flow conditions versus power farms conditions. Renewable Energy, 33**,** 2186-2198.
[2] Biadgo, A. M., Simonovic, A., Komarov, D. & Stupar, S. 2013. Numerical and Analytical Investigation of Vertical Axis Wind Turbine. FME Transactions, 41**,** 49-58.
[3] Davis, B. V. Low head tidal power: a major source of energy from the world's oceans. Energy Conversion Engineering Conference, 1997. IECEC-97., Proceedings of the 32nd Intersociety, 27 Jul-1 Aug 1997 1997. 1982-1989 vol.3.
[4] Fiedler, A. J. & Tullis, S. 2009. Blade Offset and Pitch Effects on a High Solidity Vertical Axis Wind Turbine. Wind Engineering, 33**,** 237–246.
[5] Froude, R. E. 1889. On the part played in propulsion by differences of fluid pressure.
[6] Gorlov, A. 1998. Development of the helical reaction hydraulic turbine. Final technical report, July 1, 1996--June 30, 1998. Other Information: PBD: Aug 1998.
[7] Ikoma, T., Masuda, K., Fujio, S., Nakada, H., Maeda, H. & Rheem, C. K. Characteristics of Hydrodynamic Forces and Torque on Darrieus Type Water Turbines for Current Power Generation Systems with CFD Computations. OCEANS 2008 - MTS/IEEE Kobe Techno-Ocean, 8-11 April 2008 2008. 1-8.
[8] Khan, M. J., Bhuyan, G., Iqbal, M. T. & Quaicoe, J. E. 2009. Hydrokinetic energy conversion systems and assessment of horizontal and vertical axis turbines for river and tidal applications: A technology status review. Applied Energy, 86**,** 1823-1835.
[9] Khan, M. J., Iqbal, M. T. & Quaicoe, J. E. 2010. Dynamics of a vertical axis hydrokinetic energy conversion system with a rectifier coupled multi-pole permanent magnet generator. Renewable Power Generation, IET, 4**,** 116-127.
[10] Kirke, B. K. 2011. Tests on ducted and bare helical and straight blade Darrieus hydrokinetic turbines. Renewable Energy, 36**,** 3013-3022.
[11] Lazauskas, L. & Kirke, B. K. 2012. Modeling passive variable pitch cross flow hydrokinetic turbines to maximize performance and smooth operation. Renewable Energy, 45**,** 41-50.
[12] Li, C., Zhu, S., Xu, Y.-L. & Xiao, Y. 2013. 2.5D large eddy simulation of vertical axis wind turbine in consideration of high angle of attack flow. Renewable Energy, 51**,** 317-330.
[13] Marie, D. G. J. 1931. Turbine having its rotating shaft transverse to the flow of the current. Google Patents.
[14] Marten, D., Wendler, J., Pechlivanoglou, G., Nayeri, C. N. & Paschereit, C. O. 2013. QBlade v0.6. Berlin, Germany.
[15] Niblick, A. L. 2012. Experimental and Analytical study of Helical Cross-Flow Turbines for Tidal Micropower Generation System. Master fo Science in Mechanical Engineering, University of Washington.
[16] Paraschivoiu, I. & Delclaux, F. 1983. Double multiple streamtube model with recent improvements (for predicting aerodynamic loads and performance of Darrieus vertical axis wind turbines). Journal of Energy, 7**,** 250-255.
[17] Rankine, W. J. M. & Architects, I. O. N. 1865. On the Mechanical Principles of the Action of Propellers.
[18] Rossetti, A. & Pavesi, G. 2013. Comparison of different numerical approaches to the study of the H-Darrieus turbines start-up. Renewable Energy, 50**,** 7-19.
[19] Sheldahl, R. E. & Klimas, P. C. 1981. Aerodynamic characteristics of seven symmetrical airfoil sections through 180 degree angle of attack for use in aerodynamic analysis of vertical axis wind turbines. Unlimited Release.

[20] Shino, M., Suzuuki, K. & Kiho, S. 2002. Output Characteristics of Darrieus Water Turbine with Helical Blades for Tidal Current Generations. Proceedings of The Twelfth (2002) International Offshore and Polar Engineering Conference. Kitakyushu,Japan.
[21] Strickland, J. H. 1975. The Darrieus turbine: A performance prediction model using multiple streamtubes. Albuquerque, NM: Sandia National Laboratories.
[22] Yang, B. & Shu, X. W. 2012. Hydrofoil optimization and experimental validation in helical vertical axis turbine for power generation from marine current. Ocean Engineering, 42**,** 35-46.
[23] Zhang, X.-W., Wang, S.-Q., Wang, F., Zhang, L. & Sheng, Q.-H. 2012. The hydrodynamic characteristics of free variable-pitch vertical axis tidal turbine. Journal of Hydrodynamics, Ser. B, 24**,** 834-839.